Advances in Automobile Engineering
ISSN: 2167-7670

Saad and Bari, Adv Automob Eng 2014, 3:1
DOI; 10.4172/2167-7670.1000106

Research Article Open Access

Optimizations of Vane Height of Guide Vane Swirl and Tumble Device to Improve in Cylinder Airflow Characteristics of a Diesel Engine Running with Vegetable Oil

Idris Saad[1,2]* and Saiful Bari[1]

[1]School of Engineering, University of South Australia, Mawson Lakes Campus, SA, 5095, Australia
[2]Automotive Research and Testing Center (ARTeC), Universiti Teknologi MARA, 40450, Shah Alam, Selangor, Malaysia

Abstract

Generally, compression ignition engine operating on neat vegetable oil and its blend with diesel fuel experience a reduction of engine performance and increase in exhaust emissions due to higher viscosity and lower volatility of vegetable oil than diesel fuel. Vegetable oil is less prone to evaporate, diffuse and mix with the in-cylinder air which eventually reduces the combustion efficiency and produces more emissions of CO and unburned HC. Therefore, this research investigated the potential of guide vane swirl and tumble device (GVSTD) to guide the air entrance to create more organized turbulence inside the fuel injected region to enhance the mixing process of air and vegetable oil. In order to do so, a base model of 3D computational fluid dynamic of internal combustion engine simulation was developed, verified and then simulations were carried with different GVSTD models. The results of turbulent kinetic energy, velocity, vorticity and swirling strength were compared to determine the optimum vane height. This research found that the 2 mm vane height was the optimum vane height with 35° twist angle, four vanes being arranged perpendicularly to each other and 30 mm vane length. Other different heights of vanes also showed improvement but 2 mm height showed the highest number of improvements. This could be due to the airflow pattern in bowl-in-piston head shape was amplified by the airflow pattern produced by the guide vane of 2 mm vane height. The extra turbulence, swirl, vorticity and velocity in the fuel injected region created by the 2 mm height vane is expected to enhance the mixing of vegetable oils with air to improve combustion and reduce CO and unburned HC emissions.

Keywords: Neat vegetable oil; Guide vanes; Diesel engine; Airflow; CFD

Abbreviations: CA: Crank Angle; CI: Compression Ignition; GVSTD: Guide Vane Swirl and Tumble Device; PM: Particulate Matter; SOC: Start of Combustion; SOI: Start of Injection; SI: Spark Ignition; SST: Shear Stress Transport; TDC: Top Dead Center; ρ: Fluid Density; P: Fluid Pressure; S_m: Momentum Source; T: Strain Rate; Λ: Thermal Conductivity; U: Three Dimensional Flow Velocities in X, Y and Z Directions; H_{tot}: Total Enthalpy; K: Turbulent Kinetic Energy; E: Turbulent Eddy Dissipation; Ω: Turbulence Frequency

Introduction

The key factor contributing to the research and development of renewable/alternative fuels is the unsettling fact that the world is currently experiencing an oil crisis with fuel prices dramatically rising. This problem became apparent in the World Energy Forum in 2009 and it was predicted that world crude oil reserves can only be sustained for less than 50 years [1,2] concurrently with increasing demand. The oil crisis was initially detected in the early 1970s [3]. Subsequently after the acknowledgement of depleting oil reserves, the trend towards searching for alternative fuels in order to mitigate this problem grew. Additionally, the emissions produced from vehicle exhaust pipes (CO_2, CO, NOx and PM) are also a major issue, especially in cities with high population densities [4-7]. The production of CO_2 is a threat to the ozone layer. CO and NOx are toxic gases that are harmful to human body. Thus, it is vital to rectify these global problems or at least reduce the dependency on petroleum based fuels due its detrimental effects.

Based on the preceding facts, the guidelines of future fuels can be summarized according to its properties such as its renewability and environmental friendliness. These two properties can be fulfilled by several types of biofuels such as methanol, ethanol, neat vegetable oil and transesterificaion of vegetable oil to biodiesel. However, due to higher viscosity and lower calorific values neat vegetable oils and biodiesel are usually blended at various proportions with diesel to run in diesel engines. These blends can be used directly in existing CI engines with minor or no modifications [1,3,8]. As a result, the current trends for research in this area, particularly for the usage, testing and improvement of neat vegetable oil and biodiesel [9-13] are dramatically increasing.

Many researchers have been carried out on diesel engines with neat vegetable oil blended with diesel fuel. Transesterificaion of vegetable and other sources to biodiesel can make properties of biodiesel much closer to diesel fuel with reduced viscosity. The cost of biodiesel is still much higher than diesel fuel [14]. Yaakob et al. [15] found that the cost of biodiesel was around 1.3 to 3 times more than diesel when they reviewed the production of biodiesel worldwide. Therefore, in many countries neat vegetable oil is blended with diesel fuel to run diesel engines. Forson et al. [9] experimented CI engine fuelled by blending 2.6%, 20% and 50% of jatropha oil with diesel fuel named as B2.6, B20 and B50, respectively. They reported that the blend B2.6 produced highest brake power and brake thermal efficiency with incremental values of approximately 0.25 kW and 4.2%, respectively at 9.2 N-m

***Corresponding author:** Idris Saad, School of Engineering, University of South Australia, Mawson Lakes Campus, SA, 5095, Australia, Tel: +603 5543 6281; Fax: +603 5543 5190; E-mail: saaiy003@mymail.unisa.edu.au

Received March 07, 2014; **Accepted** March 28, 2014; **Published** April 05, 2013

Citation: Saad I, Bari S (2014) Optimizations of Vane Height of Guide Vane Swirl and Tumble Device to Improve in Cylinder Airflow Characteristics of a Diesel Engine Running with Vegetable Oil. Adv Automob Eng 3: 106. doi:10.4172/2167-7670.1000106

torque as compared to diesel fuel. As for specific fuel consumption, a significant reduction of approximately 10.6% was reported. However, the engine operating on 100% jatropha oil had the lowest engine efficiency, brake power and highest fuel consumption compared to fuels that were blended with diesel. Bari et al. [10] preheated palm oil up to 60°C to lower its viscosity and be at par with the viscosity of diesel fuel. Their combustion analysis found 6% increment of peak pressure and a shorter ignition delay of 2.6°CA from diesel fuel. However, the exhaust emissions showed increments of CO and NO emissions of 9.2% and 29.3%, respectively over the entire load range. Another research from Bari et al. [11] proved that by advancing 4°CA injection timing, the engine efficiency increased by approximately 1.6% and CO emission reduced by approximately 9.9% for direct injection diesel engine running on waste cooking oil. The engine however, incurred a considerable production of NO emissions with a 76% increment. Additionally, durability tests of an engine running with palm oil were performed by Bari et al. [12] and the results were compared for short and 500 hour runs operations. For the short term engine test, they found that the peak engine pressure increased by about 5% while the ignition delay was shorter by about 3°CA compared to diesel fuel. However after 500 hours of operation, the maximum engine power experienced a reduction of about 20% and the engine consumed an extra 20% fuel. Furthermore, after the engine was dismantled, carbon deposits were found in the combustion chamber. Rakopoulos et al. [16] compared the environmental behaviour of bus diesel engine operating on blends of diesel fuel with four straight vegetable oils; sunflower, cottonseed, corn and olive oils at ratios of B10 and B20. Generally all blends produced extra unburned hydrocarbon (HC) in the range between 4 and 20% than diesel fuel. Rakopoulos et al. [16] blamed the higher viscosity of the blends as the main reason to produce higher unburned HC. According to in-cylinder CI engine combustion theory [17,18] the production of HC is due to the incomplete combustion when the fuel is not mixed properly with the in-cylinder air. Hence, proper mixing is needed to solve or at least reduce the unburned HC emission. Based on the above discussion, the preceding researches portray the colours of engines running on neat vegetable oil and it can be concluded that up to as of now, further research is required in order to make an engine perform satisfactorily with neat vegetable oil even when blended with diesel fuel.

The drawbacks mentioned above are mainly due to higher viscosity, lower volatility and heavier molecules present in neat vegetable oils [19-22]. This phenomenon reduces the ability of the fuel to evaporate and mix with the air; consequently this mitigates the combustion efficiency and affects various other parameters as mentioned earlier. Most of the researchers have concentrated on improving the combustion with neat vegetable oil by preheating or blending neat vegetable oil with diesel. These methods improved the combustion with reductions of CO emission and unburned HC but they are still higher than diesel fuel. Also, durability test still showed carbon deposits inside the combustion chamber. This is due to lower volatility and heavier molecules present in neat vegetable oil. Therefore, this research attempts to improve the characteristic of in-cylinder airflow by utilizing a Guide Vane Swirl and Tumble Device (GVSTD) since so far none of the research found to do so. The GVSTD is actually a set of vanes arranged accordingly and installed in front of the intake port to develop an organized turbulent flow throughout the duration of the injection and combustion periods. This concept is actually adapted from the SI engine [23-26] where it is reported that it can enhance air-fuel mixing and can eventually improve the combustion efficiency and SI engine performance. Since the air intake systems of the SI and CI engines are similar [17,18], this research believes the proposed method can be successful to generate extra swirl and turbulence inside the fuel injected region to breakup higher viscous and heavier molecules of neat vegetable oil to be operated in CI engines.

In order to investigate the capability of the GVSTD to generate better characteristic of in-cylinder airflow, cold flow 3D computational fluid dynamics (CFD) analyses of IC engine simulation were developed. First, the base model was created to acquire the base data. Then the simulation result was verified with the experimental data before the GVSTD model was imposed in front of intake port. These data were then compared to analyse the effects of guide vanes. However, the available swirl generator patterns [23-28] for the SI engine showed that four main parameters: the height, angle, number and length would determine the optimum design of the GVSTD. Therefore, parametric optimization technique was used to determine the best design of the GVSTD. However, this research was done to determine the optimum height of the guide vane while the other parameters such as vane angle, number and length were obtained from the previous research works by the authors with some changes on the simulation model to make a model closer to the design of HINO W04D diesel engine [29-32]. This will allow deeper discussion presented in this paper about the effects of vane height to generate better in-cylinder airflow.

The results of turbulent kinetic energy (TKE), velocity, vorticity and swirling strength were compared to determine the optimum height of the GVSTD vane. With the improvement shown by the GVSTD to the in-cylinder airflow characteristics especially inside the fuel injected region, it is believed that CI engines utilizing this method will improve its performance when operating on neat vegetable oil and its blend with diesel fuel.

Considering that this research is a preliminary study to improve the performance of CI engine run with vegetable oil using guide vane to improve the in-cylinder air flow characteristics, the scope of this research is limited to the simulation and comparison of the results with the available data from other research works only. This will allow to optimize the design of GVSTD to limit the unnecessary fabrication of many models which is time- consuming and expensive [33]. The detail of simulation method and results are explained in the following sections.

Simulation Model

The geometry of the simulation model was adapted from a HINO W04D diesel generator engine and the engine specifications are given in Table 1. This research assumed that the intake air was equally distributed among the four cylinders. Hence, the simulation model only considered single cylinder for the analyses to reduce the complexity of the simulation because the fluid flow in an IC engine is associated with large density variations and considered as one of the most challenging fluid dynamics problems to model [34,35]. Six components: intake runner, intake port, intake valve, cylinder, exhaust valve and exhaust port were drawn using SolidWorks2012 software and assembled together before being transferred into ANSYS Design Modeller to assign its materials. A Solid domain was set for both valves while a fluid domain was set for other components. Figure 1 illustrates the simulation model without GVSTD and is known as the base model denoted as 0.00R.

The GVSTD was designed according to the inspired idea from the published pattern [23-28] for SI engines. Based on that, it can be summarized that the design of the GVSTD depends on four main

Technical Specifications	
Engine Model	HINO40WD
Bore×Stroke	10^4×10^8 mm
Intake Air	NaturallyAspirated
Intake Diameter	80 mm
Number of Cylinders	4
Compression Ratio	17.9
Engine Speed	1500 rpm
Intake Valve Open	16^{0}b TDC
Intake Valve Close	40^{0}a BDC
Exhaust Valve Open	55^{0}b BDC
Exhaust Valve Close	13^{0}a TDC
Type of Piston Head	Bowl-in-Piston
Start of Fuel Injection (SOI)	14^{0}bTDC

Table 1: Basic technical specifications of the engine.

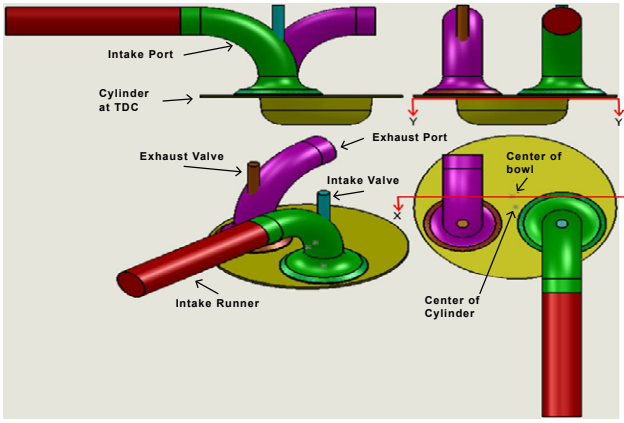

Figure 1: The drawing of base model-0.00R.

Parameters	Value
Number of Vanes (N)	4 vanes equally spaced
Vanes Twist Angle (θ)	350 Clock wise direction
Radius of Intake Runner(R)	10 mm
Length of Vane (l)	3R
Height of Vane (H)	0.10R, 0.20R, 0.30R, 0.40R, 0.50R
0.60R, 0.70R, 0.80R, 0.90R, 1.00R	
Note: #Rrepresents the number multiply by 10 mm of intake radius. Examples: 0.40R=0.40x10 mm=4 mm	

Table 2: Specification of GVSTD.

parameters which are vane height, angle, length and number. As explained earlier, the optimization was limited to the vane height while the vane twist angle, length and numbers were taken from the previous research works by the authors [29,30,36] and fixed at 35° twist angle, length three times the intake radius (3R) and four vanes arranged perpendicularly to each other. In this research, the GVSTD vane height was varied from 10% to 100% of the intake radius (R) with an increment of 10%. The specification of GVSTD is tabulated in Table 2 and it is a sample of the 0.70R GVSTD with its assembly shown in Figure 2.

Model Formulation

The IC engine simulations covered the cold air analysis within the 3D region and were solved by using ANSYS-CFX 14.0. The governing equations including continuity, momentum and energy equations [37] were used to calculate the fluid flow and are given as equations (3.1), (3.2) and (3.3), respectively and their symbols can be referred to in the list of symbols.

$$\frac{\partial \rho}{\partial t} + \nabla.(\rho U) = 0$$

$$\frac{\partial (\rho U)}{\partial t} + \nabla.(\rho U \times U) = -\nabla_P + \nabla.\tau + S_M$$

$$\frac{\partial (\rho h_{tot})}{\partial t} - \frac{\partial \rho}{\partial t} + \nabla.(\rho U h_{tot}) = \nabla.(\lambda \nabla T) + (\nabla.\tau) + U.S_M$$

Since this project aims to examine the turbulent flow generated by guide vanes which includes near wall region, shear stress transport (SST) model was used in this simulation to calculate the turbulent flow. This model combines the advantages of the K-ε model in the outer region of the exterior of the boundary layer with what the K-ω model does best in the inner boundary layer by using eddy viscosity model [37-39]. Basically, the eddy viscosity model has a deficiency as compared to Reynolds stress model for simulating high swirl, however it is still considered as the best compromise between computational time and precision [40]. Because of that the eddy viscosity model was widely used in the area of simulating the in-cylinder air flow [35,40-43].

The simulation was performed from 0°CA up to 1440°CA, which covers two cycles. This condition was required because it was arduous to set the actual values of the initial conditions of simulation. Hence at the beginning of the simulation (0°CA), the initial value for velocity, pressure and temperature were set at 0 m/s, 1 atm. and 300 K respectively and the simulation was performed until the completion the first cycle. The values were then transferred into the second cycle and continuously ran until the completion of the second cycle. The residual target for the convergence criteria was set at 1×10^{-4} to satisfy the discretised equations. For this setting, the convergence control was set at minimum and maximum coefficient loops of 1 and 500, respectively.

Results and Discussions

The main objective of this project is to determine the optimum height of the GVSTD vanes to provide better in-cylinder air-flow characteristic which will improve the air-fuel mixing which will then eventually improve combustion and engine performance. Before the

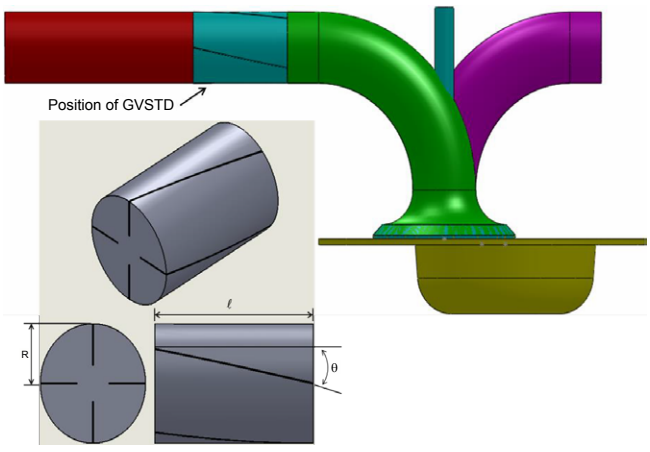

Figure 2: GVSTD–0.70R and its assembly.

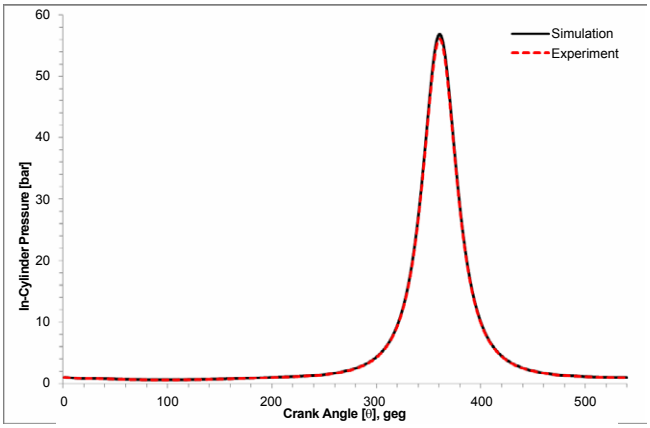

Figure 3: In-Cylinder Pressure versus Crank Angle.

simulations were performed with the GVSTD, the in-cylinder pressure of the base model was verified with the in-cylinder pressure developed by the HINO W04D diesel engine driven at 1500 rpm. The GVSTD models were then simulated and their results were analyzed.

Four main parameters of the in-cylinder airflow such as turbulent kinetic energy (TKE), velocity, vorticity and swirling strength were examined before the optimum vane height of the GVSTD was determined. These parameters were observed at five positions: 5°CA before the Start of the Injection (SOI), SOI, Start of Combustion (SOC), Top Dead Center (TDC) and 5°CA after TDC for their average and maximum values. Based on Table 1, SOI for HINO W04D diesel engine is 14° bTDC and according to different sources the ignition delay period for typical CI engine is about 6° crank angle [11,17,18]. Hence data were recorded at 341°, 346°, 352°, 360° and 365° crank angle (i.e., at 5 crank angles). In total for each model there are 40 data which consist of average and maximum values of four parameters of TKE, velocity, vorticity and swirling strength at those 5 crank angles. Moreover, this paper also presents the results in term of contours and vectors to visualize the in-cylinder portrait of those variables. However, in order to focus the discussion toward the very relevant data and avoid lengthiness of this paper, only selected contour and vectors are presented. The cut view planes to plot the contours and vectors can be referred to Figure 1 and denoted as Y–Y and X–X for top and front views respectively. Those contours and vectors are plotted when the cylinder is at SOI because this point is considered to be the critical point to break up the higher viscous injected fuels.

Model validation

The HINO W04D diesel engine was driven at 1500 rpm. A Water-cooled piezoelectric Kistler 7061B pressure sensor, TDC position optical sensor and magnetic pickup shaft encoder were installed into the engine and used to determine the in-cylinder pressure and crank angle data of the engine. To convert the output electrical charge from piezoelectric pressure sensor into DC voltage, a Kistler 5007 charge amplifier was used. From this amplifier, the analogue outputs signal were received and then converted into digital data via a data acquisition card to ensure continuous data were suitable to be managed by a laptop. The outflow data from the charge amplifier, shaft encoder and TDC position sensor were then monitored and saved by using the Lab View 7.1 software. The result of in-cylinder pressure from this experiment for one complete cycle from 0°CA until 720°CA is plotted in Figure 3. The in-cylinder pressure from the simulation of 0.00R with the same range of CA is superimposed on the graph. Generally, both results show a similar pattern where the peak pressure occurs at the TDC since there is no fuel injection and combustion involved. Both graphs are in adequate agreement but the values of in-cylinder pressure from experiment were slightly lower than simulation. This was expected due to the leakage of the gas from the cylinder to the crankcase which was not considered in the case of simulation. Bottone et al. [44] compared the in-cylinder pressure of the experimental motored CI engine with the simulation using STAR-CD commercial CFD package. They also found that the peak pressure for both results occurred at TDC. Furthermore, the result of in-cylinder pressure from the experiment was slightly lower than the simulation. They also explained that this condition was due to the leakage of the gas between piston ring and cylinder. Comparing the results from their study and this research, both are found in the same line. Similar behavior of in-cylinder pressure versus crank angle was also presented by Rakopoulos et al. [45] in their study about the effect of crevice flow in internal combustion engines using a new simple crevice model executed by a CFD code.

In-cylinder Turbulence Kinetic Energy (TKE)

Turbulent kinetic energy (TKE) is defined as the mean kinetic energy per unit mass associated with eddies in turbulent flow [46]. The in-cylinder TKE will help break up and disperse the fuel molecules during the fuel injection and evaporation periods before the combustion occurs. Higher in-cylinder TKE of air is expected to accelerate this process than normal condition of TKE for neat vegetable oil since neat vegetable oil possesses higher viscosity and lower volatility. Figure 4 presents the results of in-cylinder TKE at various crank angles from 341°CA i.e., before the SOI until 365°CA i.e., after TDC for the average and maximum values. Based on the results presented in Figure 4, the highest TKE for the average and maximum values were found at 341°CA and declined until 365°CA which can also be found from Figure 5. Payri [42] investigated the CFD modelling of the in-cylinder flow in direct-injection diesel engines by using a PISO algorithm. They validated the results by using laser Doppler velocimetry (LDV) on a 4-valve direct injection diesel engine. They found that the results from the CFD simulation of turbulence decayed almost linearly as it approached the TDC and they also found that this result was in an adequate agreement with their experiment. Similar patterns of TKE was also observed by Prasad [43] when they compared the swirl of various shapes of piston bowls by using the results from the simulation operating with the AVL Fire CFD software. The TKE for all the models declined linearly after 330°CA. The pattern of TKE which declined linearly not only reported by Payri [42] and Prasad [43] but also by other researchers [47] as well. By comparing the pattern of TKE and the shape of average TKE from 341°CA until 365°CA for various models as illustrated in Figure 5, it can be concluded that an appropriate agreement with the results of other researchers is achieved.

As for the average TKE in Figure 4, only 0.20R and 0.90R are better than the base model. However, the maximum TKE for 0.10R and 0.20R are better than the base model from 341°CA until TDC only. As for 0.60R, 0.80R and 0.90R, their maximum TKE are better than the base model for the entire range of analyses. Based on this graph, GVSTD 0.90R improved all ranges of data analyzed followed by GVSTD 0.20R with eight points from the total of ten observed data.

Since GVSTD 0.20R and 0.90R provided better results in the above discussion, further investigation of the contours are shown on both models compared to 0.00R and illustrate in Figure 6. Based on this figure, larger area (marked in circle) of higher TKE (shown as red colour) is seen in 0.20R as compared to 0.00R and 0.90R. The higher

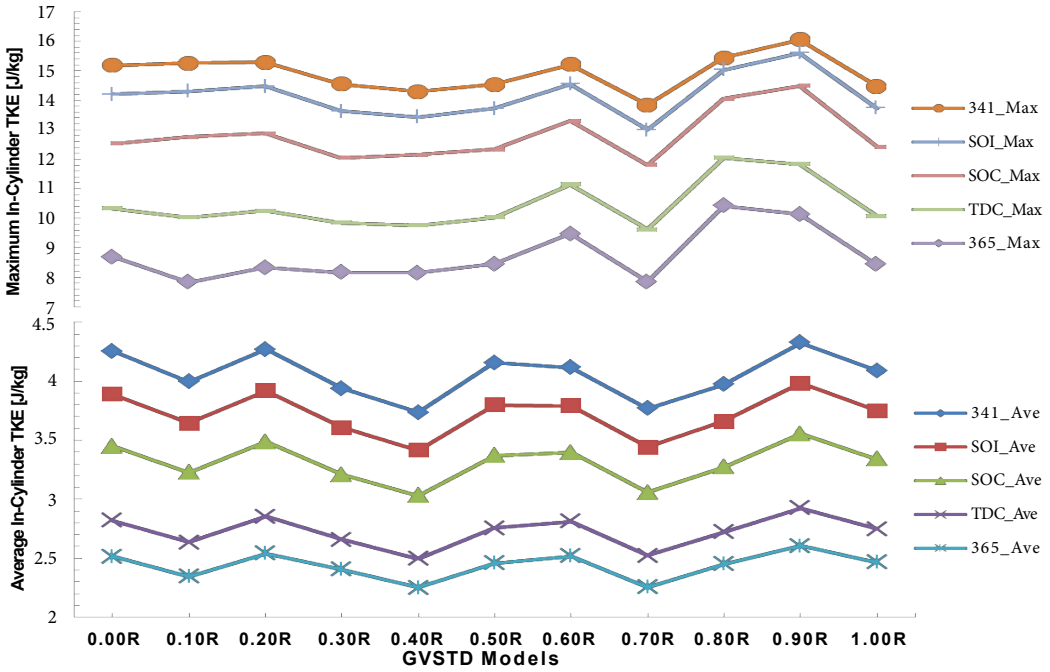

Figure 4: Maximum (top) and average (bottom) values of in-cylinder TKE of all models at 341°CA, SOI, SOC, TDC and 365°CA.

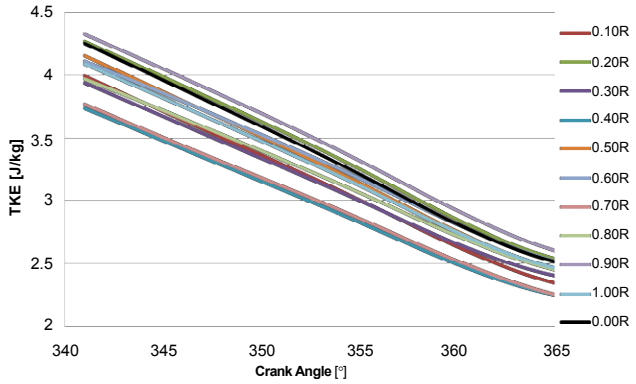

Figure 5: Average in-cylinder TKE from 341°CA to 365°CA for all models.

TKE region for 0.90R has been shifted away from the centre of the bowl. However, 0.20R shows the higher TKE region is in the centre of the bowl which is essential as the fuel is injected in this region.

The fuel is usually injected at the centre of the combustion chamber. However, for vegetable oil which is higher viscosity there is a tendency of higher penetration length and lower cone angle of the injected fuel. This causes the fuel molecules to stick to the surface of piston bowl and produced carbon deposits as observed by researchers [12,48]. This also increases the unburned HC and CO emissions of the engine.

The condition of TKE with guide vanes especially for 0.20R will definitely help breaking up higher viscosity molecules of vegetable oil due to higher TKE present in the fuel injected region. Observation made from front view of Figure 6 clearly shows that 0.20R has larger area of higher TKE (shown as red colour) near the wall of the piston bowl than 0.90R and 0.00R. This condition is expected to disperse injected fuel more and prevent the injected fuel to adhere to the surface of the bowl. Additionally, due to higher TKE higher viscosity of vegetable oil will break up more and mix with air. This will result in better combustion with reduction of unburned HC and CO emissions.

In-cylinder velocity, vorticity and swirling strength

For satisfactory in-cylinder combustion however, it is crucial that the fuel molecules mixes adequately with the air. The mixing process is augmented by the in-cylinder velocity, vorticity and swirling strength. Therefore, Figures 7-9 illustrate the average and maximum values of these parameters for the purpose of analyses to determine the best GVSTD model compared to the base model.

For the average in-cylinder velocity (Figure 7), 0.20R improved three of the five analyzed data which were at 345°CA, SOI and TDC. However the average in-cylinder velocity of 0.60R, 0.80R and 0.90R were better than the base model for the whole analyzed data. As for the maximum velocity (Figure 7) at 341°CA, all GVSTD models exceeded the base model. However, only 0.60R and 0.80R had an improvement for the entire range of analyses.

The velocity vectors of 0.00R, 0.20R and 0.90R from top and front views are presented in Figure 10 because these models provided better TKE compared to 0.00R and other GVSTD models as discussed earlier. Circles of same diameter are drawn at the centre of the bowl where the fuel is expected to be injected. From the top view of the figure, it is detected that 0.20R provided higher velocity inside the circle as compared to other models. This is the region where the fuel is expected to be injected.

Additionally, front view of Figure 10 shows the tumble generated inside the bowl of the piston. Tumble is the movement of the cylinder charge from the upside to the down side of the cylinder regions and back again, around an axis perpendicular to the cylinder axis [49]. Based on that figure, the highest velocities were generated from both top sides of the piston bowl. This condition is known as squish effect

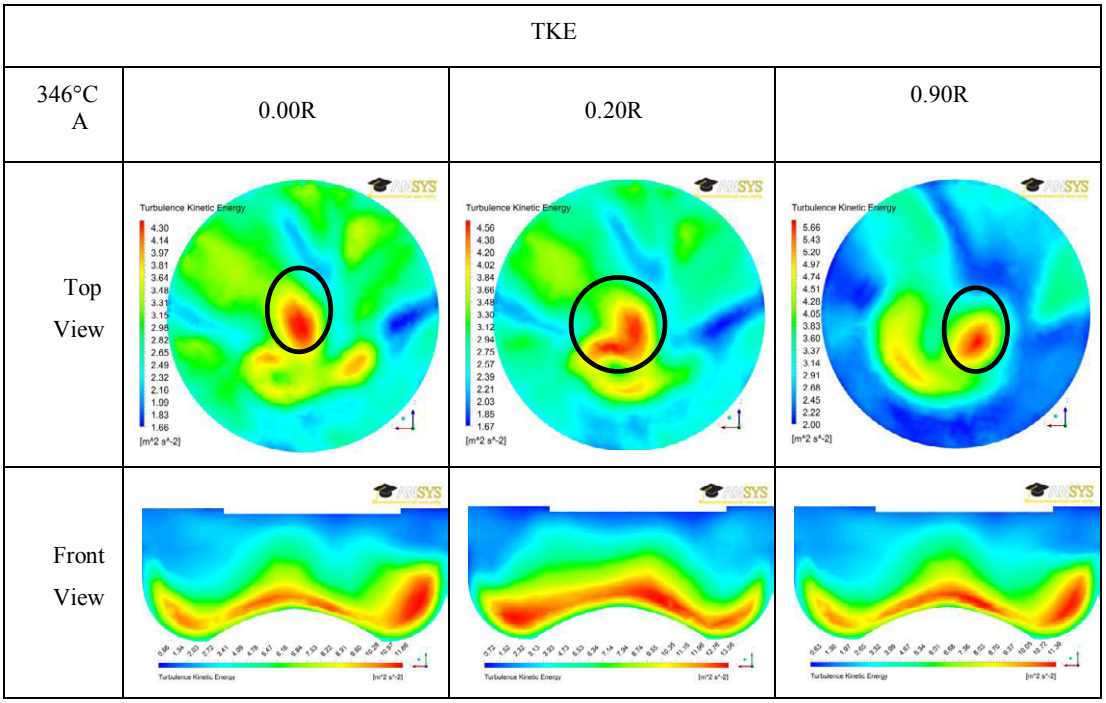

Figure 6: Comparison of top and front views of TKE contours of 0.00R, 0.20R and 0.90R at 346°CA.

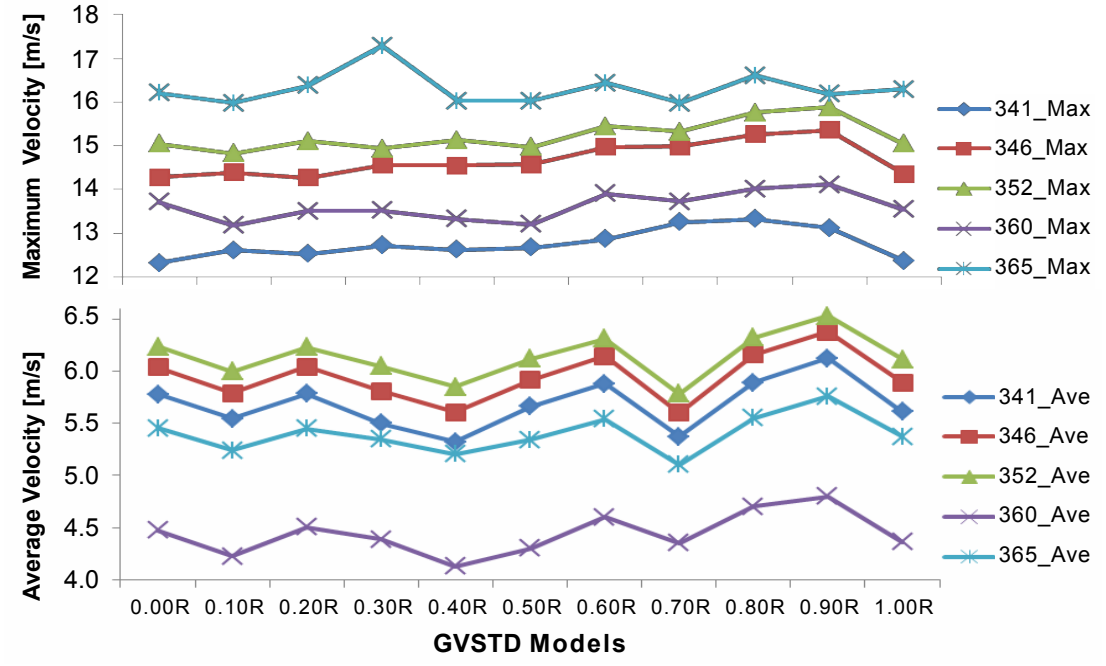

Figure 7: Maximum (top) and average (bottom) values of in-cylinder velocity of all models at 341°CA, SOI, SOC, TDC and 365°CA.

[17]. This squish effect was also observed by Sridhar et al. [40] when simulating IC engine using CFD code CFX-4.3. Rectangular boxes were drawn in the figure to demonstrate the critical area of the tumble to enhance breaking up and mixing with air of higher viscous vegetable oil based fuels. As seen from the figure, the tumble of 0.00R shown as white line indicates no velocity in that particular area. Conversely, both GVSTD models show higher tumble than 0.00R. Hence, GVSTD will give better in-cylinder tumble and increase the chances of mixing of vegetable oil with air.

Generally, vorticity is defined as the rotation of a fluid particle around a local axis [50] and it is measured as twice the angular velocity of a fluid particle [46,50,51]. Therefore, in a particular area higher

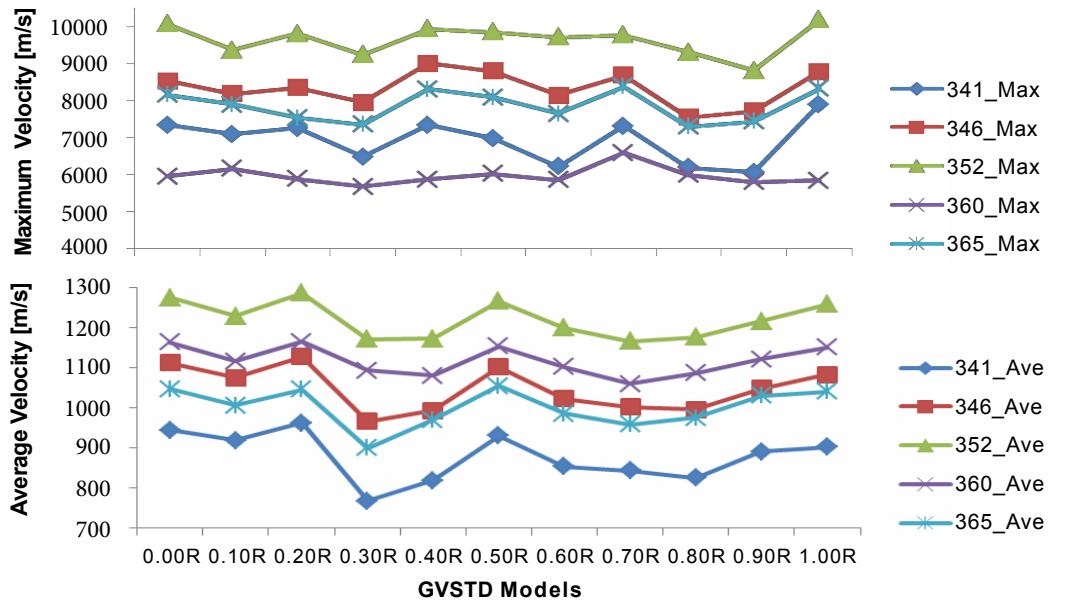

Figure 8: Maximum (top) and average (bottom) values of in-cylinder vorticity of all models at 341°CA, SOI, SOC, TDC and 365°CA.

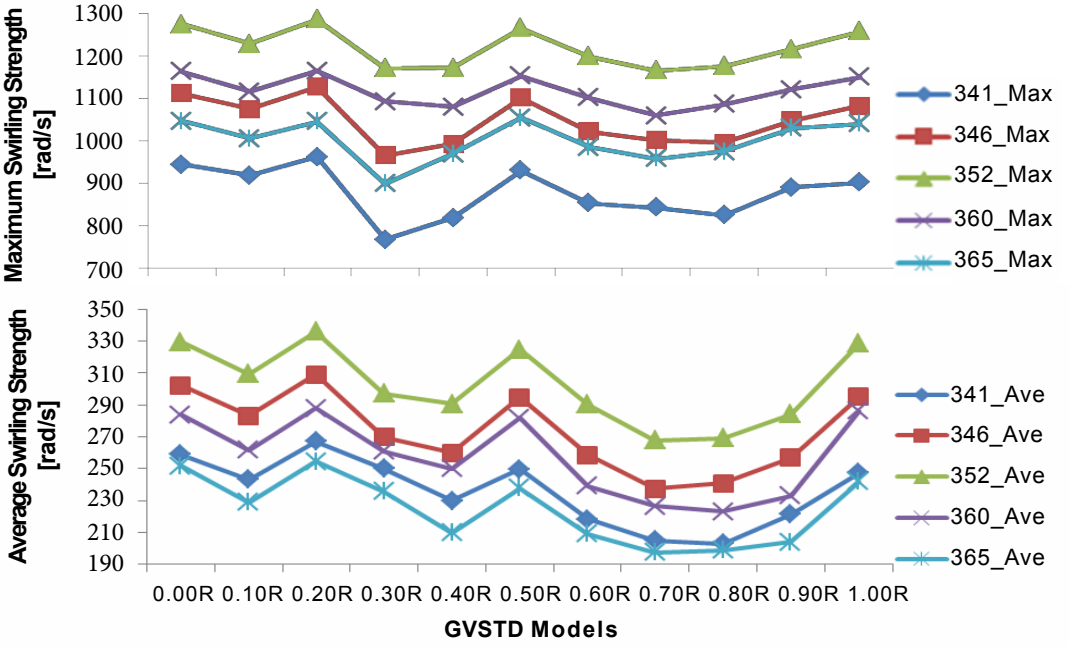

Figure 9: Maximum (top) and average (bottom) values of in-cylinder swirling strength of all models at 341°CA, SOI, SOC, TDC and 365°CA.

vorticity represents higher angular velocity in that particular area. Vorticity would be very useful to break up higher viscous vegetable oil if appropriate vorticity can be created in the fuel injected region. Figure 8 shows that only 0.20R had an improvement of average vorticity over the base model until TDC whereas the rest of the data displayed a reduction. It could be due to the vorticity generated by the GVSTD did not coincide with the vorticity generated by the bowl-in-piston which resulted in reduction of vorticity with other guide vanes except for the case of 0.20R GVSTD. However, all GVSTDs did improve the maximum vorticity (Figure 8). Combining the results of average and maximum in-cylinder vorticity, 0.20R and 1.00R provided better vorticity than other models. Therefore, vorticity vectors of 0.20R and 1.00R are compared with 0.00R for further examinations and presented in Figure 11. In top view, the vorticity regions are marked with circles in the figure. Larger area of vorticity has been detected for the case of 0.20R than 1.00R and 0.00R. Front view of Figure 11 also shows higher

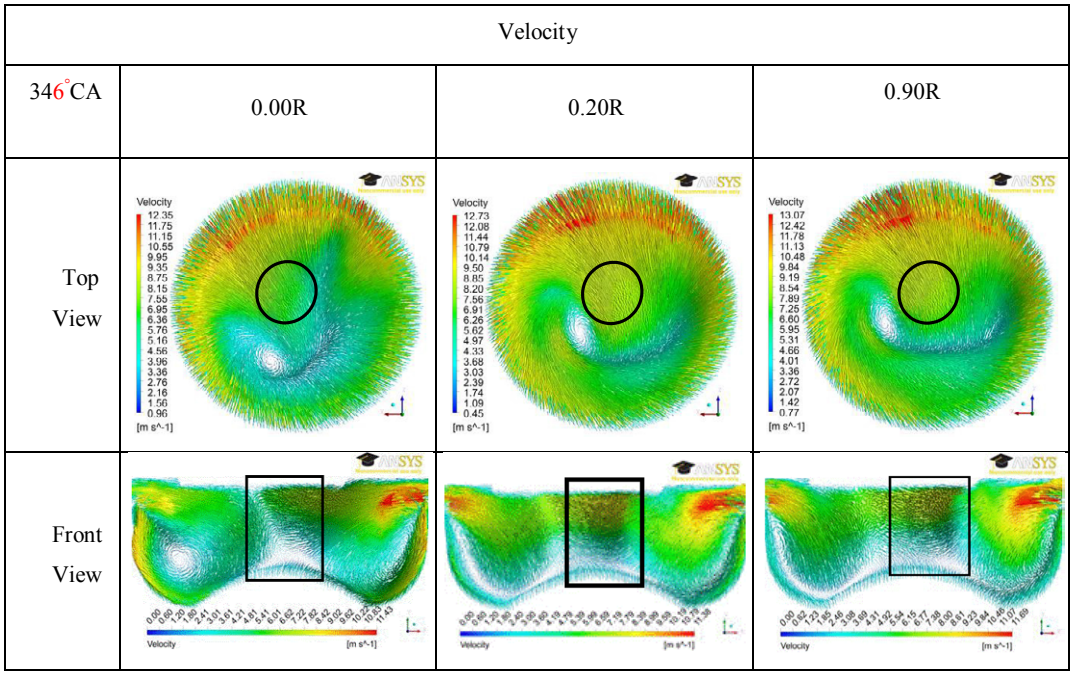

Figure 10: Comparison of top and front views of velocity vectors of 0.00R, 0.20R and 0.90R at 346°CA.

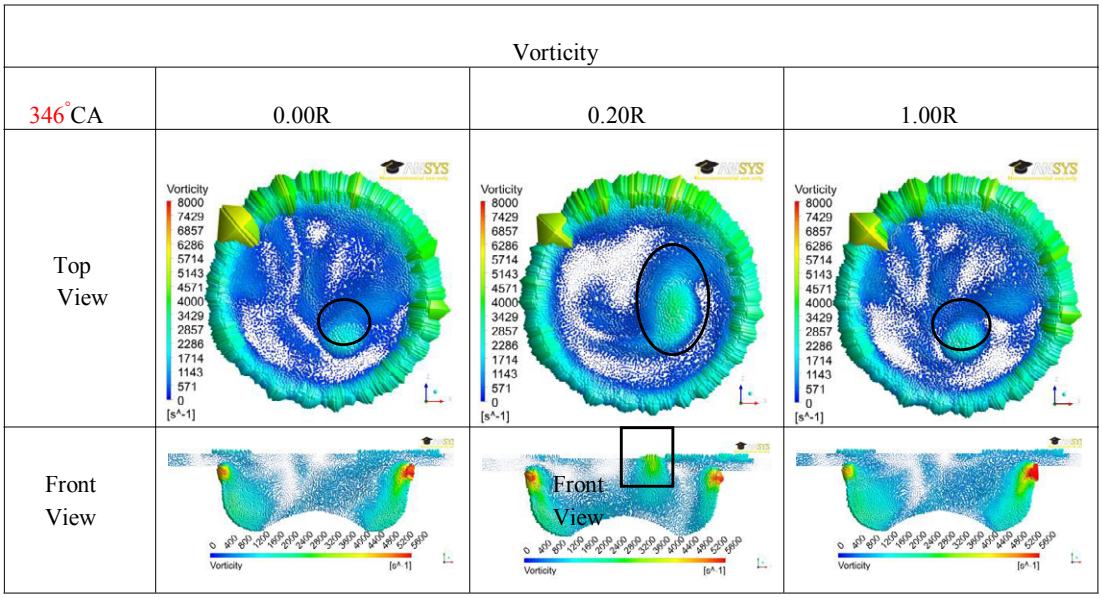

Figure 11: Comparison of top and front views of vorticity vectors of 0.00R, 0.20R and 1.00R at 346°CA.

GVSTD models	Total Increment per 40 data
0.10R	8
0.20R	24
0.30R	5
0.40R	9
0.50R	7
0.60	17
0.70	10
0.80	16
0.90	21

Table 3: Total increments made by all GVSTD models.

vorticity in the fuel injected region marked as rectangle for the case of 0.20R than 1.00R and 0.00R. This will again enhance the mixing process of air and fuel, and accelerate the combustion process.

The result for average swirling strength (Figure 9) were similar to the average vorticity where only 0.20R indicated an improvement but this time it covered the whole range of analyses. GVSTD 1.00R also gave an improvement but just for the last two observed data only. For the maximum swirling strength GVSTD 0.40R has an improvement at 341°CA, SOC, TDC and 365°CA. Also, 0.50R, 0.70R and 1.00R are better than 0.00R for the three out of five observed points. On the other

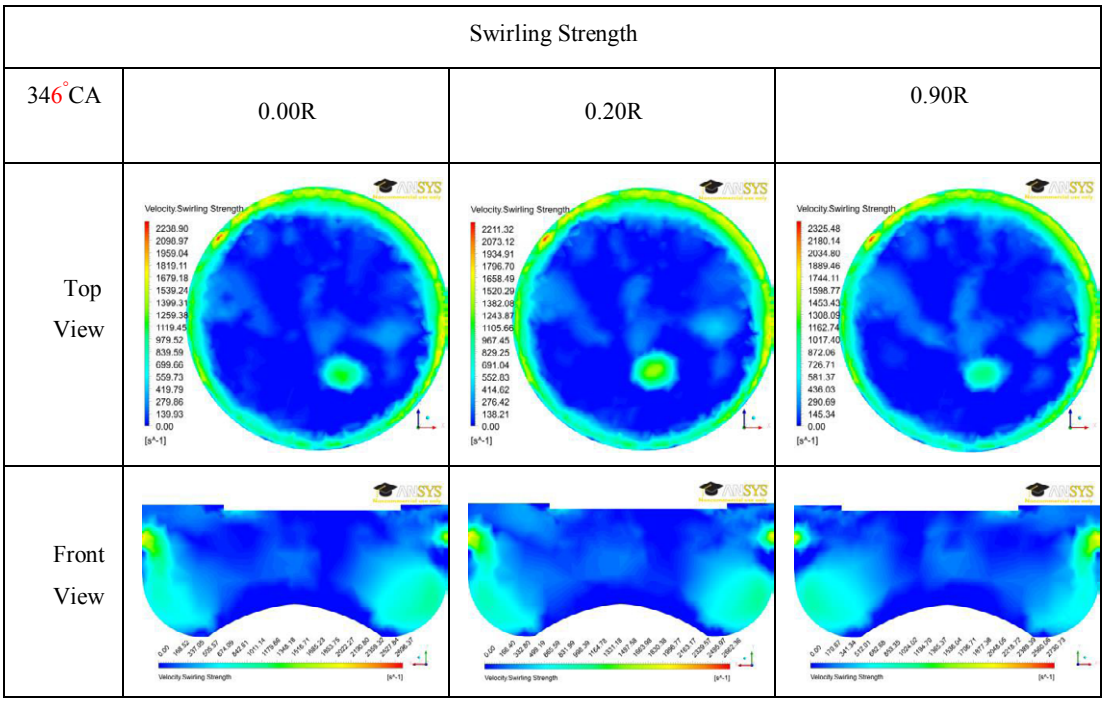

Figure 12: Comparison of top and front views of swirling strength contours of 0.00R, 0.20R and 346°CA.

hand 0.20R improved the maximum swirling strength than 0.00R after TDC. Considering the average and maximum values of swirling strength, 0.20R and 1.00R improved 6 and 5 out of 10 data, respectively and their contours are compared with 0.00R for further studies and plotted in Figure 12. The figure shows that 0.20R provide higher swirling strength marked as circle as compared to 0.90R and 0.00R.

With the results of velocity, vorticity and swirling strength provided under this section, this research is expected that the GVSTD of 0.20R will improve the performance of the diesel engine operating on vegetable oil. This is underpinned by many researchers to improve the mixing and combustion processes [23,26,43,52,53].

Optimum height of GVSTD vane

Four parameters at five different crank angles are presented above to analyse the in- cylinder airflow characteristics from 5? CA before the SOI until the earlier stage of expansion. Both the average and maximum values are included. Altogether, the total number of analyzed data was 40 for each model. The model which improved the highest data was considered to be the best vane height for this research. Table 3 presents the number of improvements for various GVSTD models. Based on the table, it is evidently shown that the 0.20R improved 24 out of 40 analyzed data. Thus, for this research, 0.20R GVSTD is selected as the best vane height with four vanes, length three times the intake radius and a 35° twist angle. This result was achieved because 0.20R provided the best in-cylinder airflow characteristic which probably coincided with the in-cylinder airflow characteristic of the bowl-in piston used in this research which is in agreement with the research carried out by Prasad [43].

Conclusion

Neat vegetable oil or its blends with diesel fuel at different proportions can be directly used in diesel engines with no or minor modifications. However, the quality of neat vegetable oil is relatively inferior to diesel fuel especially in the aspects of viscosity and volatility. It also possesses heavier molecules than conventional diesel fuel. These conditions result in a longer fuel penetration length and a lower cone angle during fuel injection. This consequently affects the air fuel mixing process which results in incomplete combustion and higher CO and unburned HC emissions with carbon deposits inside the combustion chamber. Various techniques can be utilized to ease these problems. Amongst them, are using neat vegetable oil blended with diesel and preheating the neat vegetable oil before injection into the cylinder. However, the engine running with neat vegetable oil and its blend with diesel fuel using above techniques still showed higher unburned HC and CO emissions than diesel fuel. Durability tests also showed carbon deposits inside the combustion chamber. Therefore, this research is done to improve the in-cylinder airflow characteristic by using GVSTD in the intake runner to improve the air-fuel mixing of higher viscous fuels.

Through simulations with ANSYS-CFX 14 CFD software, it was found that 2 mm (0.20R) height of four vanes, 30 mm in length with a 35° twist angle was the best design to improve the airflow characteristic inside the fuel injected region during the fuel injection until the expansion processes. GVSTD 0.20R improved 24 out of 40 data of in-cylinder TKE, velocity, vorticity and swirling strength. Both the average and maximum values of these parameters were higher than the base model i.e., without vanes. The others models of different heights improved the in-cylinder airflow characteristics for certain aspects, but 0.20R showed the highest number of improvements. This could be due to airflow pattern produced by the bowl-in-piston head coincided by the airflow pattern produced by the 0.20R guide vanes. Therefore, this paper concludes that GVSTD 0.20R is the optimum height to improve the performance of a diesel engine with bowl-in-piston type head operating on neat vegetable oil or other type of higher viscous fuels.

References

1. Sharma YC, Singh B (2009) Development of biodiesel: Current scenario. Renewable and Sustainable Energy Reviews 13: 1646-1651.

2. Annamalai K (2013) Respiratory Quotient (Rq), Exhaust Gas Analyses, CO_2 Emission and Applications in Automobile Engineering. Adv Automob Eng.
3. Kalam MA, Masjuki HH (2002) Biodiesel from palmoil-an analysis of its properties and potential. Biomass and Bioenergy 23: 471-479.
4. Ibrahim A, Bari S (2010) An experimental investigation on the use of EGR in a supercharged natural gas SI engine. Fuel 89: 1721-1730.
5. Ibrahim A, Bari S (2009) A comparison between EGR and lean-burn strategies employed in a natural gas Slengine using a two-zonecombustion model. Energy Conversion and Management 50: 3129-3139.
6. Ubong E (2012) Alternative Fuels and Renewable Energy Strategies in the Energy Revolution. Adv Automob Eng.
7. Bari S (2014) Performance, combustion and emission tests of a metro-bus running on biodiesel-ULSD blended (B20) fuel. Applied Energy 124: 35-43.
8. Murugesan A (2009) Bio-diesel as an alternative fuel for diesel engines-Areview. Renewable and Sustainable Energy Reviews 13: 653-662.
9. Forson FK, Oduro EK, Hammond-Donkoh E (2004) Performance of jatropha oil blends in a diesel engine. Renewable Energy 29: 1135-1145.
10. Bari S, Lim TH, Yu CW (2002) Effects of preheating of crude palm oil (CPO) on injection system, performance and emission of a diesel engine. Renewable Energy 27: 339-351.
11. Bari S, Yu C, Lim TH (2004) Effect of fuel injection timing with waste cooking oil as a fuel in a direct injection diesel engine. Proceedings of the Institution of Mechanical Engineers, Part D: Journal of Automobile Engineering 218: 93-104.
12. Bari S, Yu C, Lim TH (2002) Performance deterioration and durability issues while running a diesel engine with crude palm oil. Proceedings of the Institution of Mechanical Engineers,Part D: Journal of Automobile Engineering 216: 785-792.
13. Bari S, Roy MM (1995) Prospect of ricebranoil as alternative to diesel fuel, in Fifth International Conference on Small Engines, their Fuels and the Environment.
14. HaasM J, Andrew J McAloon, Winnie C Yee, Thomas A Foglia (2006) Aprocess model to estimate biodiesel production costs. Bioresource Technology 97: 671-678.
15. Yaakob Z (2013) Overview of the production of biodiesel from Waste cooking oil. Renewable and Sustainable Energy Reviews 18: 184-193.
16. Rakopoulos DC (2011) Comparative environmental behavior of bus engine operating on blends of diesel fuel with four straight vegetable oils of Greek origin: Sunflower, cottonseed, corn and olive. Fuel 90: 3439-3446.
17. Heywood JB (1988) Internal Combustion Engines Fundamentals. McGraw Hill International.
18. Pulkrabek WW (2004) Engineering Fundamental of the Internal Combustion Engine. Prentice Hall.
19. Carraretto Cetal (2004) Biodiesel as alternative fuel: Experimental analysis an denergetic evaluations. Energy 29: 2195-2211.
20. Benjumea PA, Gudelo J, Agudelo A (2008) Basic properties of palm oil biodiesel-diesel blends. Fuel 87: 2069-2075.
21. Ramadhas AS, Muraleedharan C, Jayaraj S (2005) Performance and emission evaluation of a diesel engine fueled with methyl esters of rubber seed oil. Renewable Energy 30: 1789-1800.
22. Bari S, Yu C, Lim T (2002) Filter clogging and power loss issues while running a diesel engine with waste cooking oil. Proceedings of the Institution of Mechanical Engineers, Part D: Journal of Automobile Engineering, 216: 993-1001.
23. Kim JS (2006) Fluid Swirling Device, in United States Patent. USA.
24. Kim JS (2003) Fluid Swirling Device for an Internal Combustion Engine, in United States Patent. USA.
25. Kim JS (2000) Air Turbulence Generator of Internal Combustion Engines, in United States Patent. USA.
26. Lin SS, Yang JC (2000) Intake Swirl Enhancing Structure for Internal Combustion Engine, in United States Patent. USA.
27. Kim SY (1990) Air Flow System for an Internal Combustion Engine, in United States Patent. USA.
28. Kim SY (1999) Air Flow System for Internal Combustion Engine, in United States Patent. USA.
29. Saad I, Bari S (2011) Effects of Guide Vane Swirl and Tumble Device (GVSTD) to the Air Flow of naturally aspirated CI engine. International Conference on Mechanical Engineering 2011 (ICME2011).
30. Saad I, Bari S (2013) Improving Air-Fuel Mixing in Diesel Engine Fuelled by Higher Viscous Fuel using Guide Vane Swirl and Tumble Device (GVSTD). SAE 2013 World Congress & Exhibition. SAE: Detroit, Michigan, USA.
31. Saad I, Bari S, Hossain SN (2013) In-Cylinder Air Flow Characteristics Generated by Guide Vane Swirl and Tumble Device to Improve Air-Fuel Mixing in Diesel Engine Using Biodiesel. Procedia Engineering 56: 363-368.
32. Bari S, Saad I (2013) CFD modeling of the effect of guide vane swirl and tumble device to generate better in-cylinder air flow in a CI engine fuelled by biodiesel. Computers & Fluids 84: 262-269.
33. El-Sayed MEM (2012) Changing Paradigms in Automobile Engineering. Adv Automob Eng 1: e101.
34. Basha SA, Raja Gopal K (2009) In-cylinder fluid flow, turbulence and spray models-Areview. Renewable and Sustainable Energy Reviews 13: 1620-1627.
35. Zhu Y (2004) Computational study of the effects of the geometry of the piston bowl pip for a high-speed direct injection diesel engine. Proceedings of the Institution of Mechanical Engineers 218: 875-890.
36. Saad I, Bari S, Hossain SN (2012) Optimum Height of Guide Vane to Improve In-Cylinder Air Flow in CI Engine Operated with Biodiesel. In 1st Biannual International Conference on Powertrain Modelling and Control (PMC2012), University of Bradford, West Yorkshire, UK.
37. ANSYS INC, CFX-Solver Theory Guide, R. 12.1, Editor. 2009.
38. Anderson JD (1995) Computational fluid dynamics: the basics with applications, McGraw-Hill, NewYork.
39. Tu J (2008) Computational fluid dynamics: a practical approach. (1st Edition). Amsterdam: Butter worth-Heinemann.
40. Sridhar G, Paul PJ, Mukunda HS (2004) Simulation of fluid flow in a high compression ratio reciprocating internal combustion engine. Proceedings of the Institutionof Mechanical Engineers 218: 403-416.
41. Jasak H (1999) Rapid CFD simulation of internal combustion engines.
42. Payri F (2004) CFD modeling of the in-cylinder flow in direct-injection Diesel engines. Computers & Fluids 33: 995-1021.
43. Prasad BVVSU (2011) High swirl-inducing piston bowls in small diesel engines for emission reduction. Applied Energy 88: 2355-2367.
44. Bottone F (2012) Large Eddy Simulation of Diesel Engine In-cylinder Flow. Flow, Turbulence and Combustion 88: 233-253.
45. Rakopoulos CD (2011) Investigating the effect of crevice flow on internal combustion engines using a new simple crevice model implemented in a CFD code. Applied Energy 88: 111-126.
46. White FM (2011) Fluid mechanics. (7thedn). McGraw Hill, New York.
47. Micklow G, Gong W (2007) Intake and in-cylinder flow field modelling of a four-valve diesel engine. Proceedings of the Institution of Mechanical Engineers, Part D: Journal of Automobile Engineering 221: 1425-1440.
48. Bari S (2004) Investigation Into the Deteriorated Performance of Diesel Engine After Prolonged Use of Vegetable Oil. ASME Conference Proceedings (37467): 447-455.
49. Jorge Martins BR, Senhorinha Teixeira (2009) In-Cylinder Swirl Analysis of Different Strategies on Over-Expanded Cycles. Proceedings of COBEM.
50. Cengel YA, Cimbala JM (2010) Fluid mechanics. (2ndedn). McGraw-Hill Higher Education.
51. Young DF (2009) Fundamentals of fluid mechanics. (6thedn). Wiley. 725: 6-13.
52. Miles PC (2000)The influence of swirl on HSDI diesel combustion at moderate speed and load. SAE International Journal.
53. Benajes J (2004) The effect of swirl on combustion and exhaust emissions in heavy-duty diesel engines. Proceedings of the Institution of Mechanical Engineers, PartD: Journal of Automobile Engineering 218: 1141-1148.